JYX JYVÄSKYLÄN YLIOPISTO UNIVERSITY OF JYVÄSKYLÄ

This is a self-archived version of an original article. This version may differ from the original in pagination and typographic details.

Author(s): Guo, Fu-Sheng; Chen, Yan-Cong; Tong, Ming-Liang; Mansikkamäki, Akseli; Layfield, Richard

Title: Uranocenium : Synthesis, Structure and Chemical Bonding

Year: 2019

Version: Accepted version (Final draft)

Copyright: © 2019 Wiley-VCH Verlag GmbH & Co.

Rights: In Copyright

Rights url: http://rightsstatements.org/page/InC/1.0/?language=en

Please cite the original version:

Guo, F.-S., Chen, Y.-C., Tong, M.-L., Mansikkamäki, A., & Layfield, R. (2019). Uranocenium : Synthesis, Structure and Chemical Bonding. Angewandte Chemie, 58(30), 10163-10167. https://doi.org/10.1002/ange.201903681

Angewandte Chemie

GDCh

Eine Zeitschrift der Gesellschaft Deutscher Chemiker

www.angewandte.de

Akzeptierter Artikel

Titel: Uranocenium: Synthesis, Structure and Chemical Bonding

Autoren: Richard Layfield, Fu-Sheng Guo, Akseli Mansikkamaki, Ming-Liang Tong, and Yan-Cong Chen

Dieser Beitrag wurde nach Begutachtung und Überarbeitung sofort als "akzeptierter Artikel" (Accepted Article; AA) publiziert und kann unter Angabe der unten stehenden Digitalobjekt-Identifizierungsnummer (DOI) zitiert werden. Die deutsche Übersetzung wird gemeinsam mit der endgültigen englischen Fassung erscheinen. Die endgültige englische Fassung (Version of Record) wird ehestmöglich nach dem Redigieren und einem Korrekturgang als Early-View-Beitrag erscheinen und kann sich naturgemäß von der AA-Fassung unterscheiden. Leser sollten daher die endgültige Fassung, sobald sie veröffentlicht ist, verwenden. Für die AA-Fassung trägt der Autor die alleinige Verantwortung.

Zitierweise: *Angew. Chem. Int. Ed.* 10.1002/anie.201903681
Angew. Chem. 10.1002/ange.201903681

Link zur VoR: http://dx.doi.org/10.1002/anie.201903681
http://dx.doi.org/10.1002/ange.201903681

WILEY-VCH

10.1002/ange.201903681

WILEY-VCH

COMMUNICATION

Uranocenium: Synthesis, Structure and Chemical Bonding

Fu-Sheng Guo,[a] Yan-Cong Chen,[b] Ming-Liang Tong,*[b] Akseli Mansikkamäki,*[c] and Richard A. Layfield*[a]

In memory of Professor Paul O'Brien CBE FRS FREng

Abstract: Abstraction of iodide from $[(\eta^5\text{-}C_5{}^iPr_5)_2UI]$ (**1**) produces the cationic uranium(III) metallocene $[(\eta^5\text{-}C_5{}^iPr_5)_2U]^+$ (**2**) as a salt of $[B(C_6F_5)_4]^-$. The structure of **2** consists of unsymmetrically bonded cyclopentadienyl ligands and a bending angle of 167.82° at uranium. Analysis of the bonding in **2** shows that the uranium 5f orbitals are strongly split and mixed with the ligand orbitals, leading to non-negligible covalent contributions to the bonding. Studying the dynamic magnetic properties of **2** reveals that the 5f covalency leads to partially quenched anisotropy and fast magnetic relaxation in zero applied magnetic field. Application of a magnetic field leads to dominant relaxation via a Raman process.

Sandwich compounds containing cyclopentadienyl (Cp) and cyclo-octatetraenyl (COT) ligands play a pivotal role in understanding the chemical bonding in f-block compounds and its implications for reactivity, spectroscopy and magnetism.[1] Organometallic sandwich compounds have yielded detailed insight into the balance of ionic and covalent factors in f-element chemistry and the important roles played by d- and f-orbitals,[2] leading to, for example, advances in catalysis[3] and small-molecule activation,[4] and in the stabilization of unusual oxidation states[5] and bonding motifs.[6]

Few f-element sandwich compounds have had greater impact than uranocene, the iconic D_{8h}-symmetric species $[U(\eta^8\text{-}C_8H_8)_2]$ in which the uranium(IV) centre has a $5f^2$ ground-state configuration.[7] Extensive investigations into uranocene and its derivatives have established that the uranium-carbon bonds possess an appreciable degree of covalent character, which derives mainly from overlap of 6d orbitals with the ligand orbitals, but with a significant contribution from the 5f orbitals.[8] Whilst other *bis*(COT) actinide compounds are known,[9] homoleptic *bis*(η^n-ligand) sandwich compounds are otherwise rare,[10] and homoleptic *bis*(η^5-cyclopentadienyl)actinide complexes are unknown. Previous work on f-element metallocenes has led to the suggestion that the $\{(\eta^5\text{-}Cp)_2M\}$ structural motif is invariably bent regardless of the metal and its oxidation state,[11] although no base-free examples are known for the actinides. The isolation of a homoleptic uranium metallocene would therefore furnish new insight into the nature of metal-ligand bonding in actinide compounds. Furthermore, such a metallocene should feature strong magnetic axiality and quantum tunneling properties, which could either assist with the design of high-performance single-molecule magnets or qubits for quantum computing, an area where lanthanides are prominent.[12] We therefore aimed to synthesize a cationic uranium(III) metallocene with the general formula $[(Cp^R)_2U]^+$, in which Cp^R is bulky cyclopentadienyl ligand capable of stabilizing a pseudo-two-coordinate geometry.

The target compound was synthesized by abstracting iodide from $[(\eta^5\text{-}C_5{}^iPr_5)_2UI]$ (**1**) using the super-electrophile $[(Et_3Si)_2(\mu\text{-}H)][B(C_6F_5)_4]$,[13] resulting in the formation of $[(\eta^5\text{-}C_5{}^iPr_5)_2U][B(C_6F_5)_4]$ ([**2**][$B(C_6F_5)_4$]), which was shown by X-ray diffraction to contain a uranocenium cation (Scheme 1).[14]

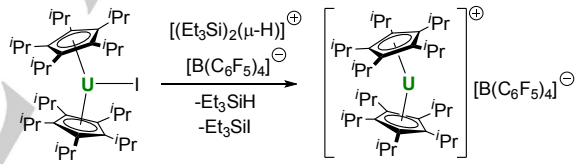

Scheme 1. Synthesis of [**2**][$B(C_6F_5)_4$].

Significant changes to structure of the metallocene unit occur upon formation of **2** from **1** (Figure 1, Table S1). In **1**, the two cyclopentadienyl ligands interact in a similar way with the uranium centre, as shown by the U–C distances, i.e. 2.767(4)-2.862(4) Å and 2.786(3)-2.854(4) Å, respectively, with associated U–Cp_{cent} distances of 2.5323(15) Å and 2.5408(15) Å (cent = centroid). The resulting Cp-U-Cp angle is 152.63(6)° and the U–I bond length is 3.0721(3) Å. In the cation **2**, one cyclopentadienyl ligand coordinates unsymmetrically to uranium, with U–C distances of 2.702(5)-2.804(6) Å and a U–Cp_{cent} distance of 2.472(3) Å. The other cyclopentadienyl ligand in **2** bonds more symmetrically, with U–C distances of 2.744(6)-2.802(6) Å and U–Cp_{cent} = 2.496(3) Å. The Cp-U-Cp angle in **2** is much wider at 167.82(8)°.

Since **2** is the first base-free actinide *bis*(cyclopentadienyl) sandwich complex, an understanding of the metal-ligand bonding in uranocenium is of importance from a fundamental perspective, whilst also providing insight into properties such as magnetism and chemical reactivity. The uranium-carbon interactions in **2** were studied by means of DFT calculations as implemented in the Amsterdam Density Functional code.[15] A schematic molecular orbital diagram for the frontier orbitals in **2** (Figure 2) shows that

[a] Dr F.-S. Guo, Prof. Dr R. A. Layfield
Department of Chemistry
University of Sussex
Falmer, Brighton, BN1 9QR (U.K.)
E-mail: R.Layfield@sussex.ac.uk
[b] Dr Y.-C. Chen, Prof. Dr M.-L. Tong
Key Laboratory of Bioinorganic and Synthetic Chemistry of the Ministry of Education, School of Chemistry
Sun Yat-Sen University
E-mail: tongml@mail.sysu.edu.cn
Guangzhou 510275 (P.R. China)
[c] Dr A. Mansikkamäki
Department of Chemistry, Nanoscience Center
University of Jyväskylä
P.O. Box 35, Jyväskylä, FI-40014 (Finland)
E-mail: Akseli.mansikkamaki@jyu.fi

Supporting information for this article is given via a link at the end of the document.

Accepted Manuscript

This article is protected by copyright. All rights reserved.

10.1002/ange.201903681

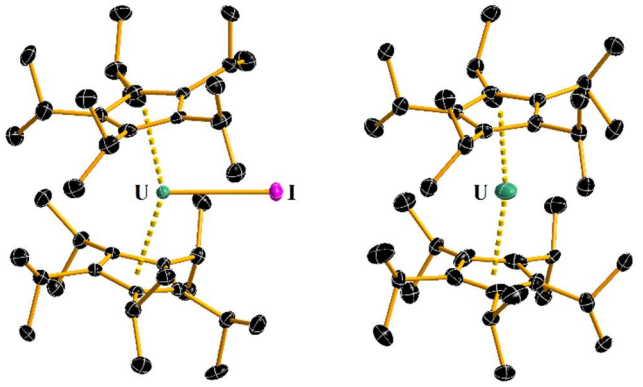

Figure 1. Molecular structure of **1** (left) and **2** (right). Thermal ellipsoids at 50% probability and hydrogen atoms omitted for clarity.

the bonding can be understood by considering the 5f and 6d orbitals of uranium(III) and the two near-degenerate π-type HOMO and HOMO–1 of the ligands. Mixing of the metal and ligand orbitals is weak in all the interactions and the bonding is dominated by electrostatics. However, covalency makes a non-negligible contribution, the main form of which is dative electron donation from the ligand HOMO and HOMO–1 to the unoccupied uranium $6d_{xz}$ and $6d_{yz}$ orbitals; the contribution from the 6d orbitals to the composition of MOs 196 and 197 varies between 14-18% (Figure S21).

The radial extension of actinide 5f orbitals allows them to contribute to covalency in metal-ligand bonds, as typified by uranocene and related compounds with η^n-bonded ligands.[2,15] In **2**, the 5f contribution to the valence orbitals is 4-8%, which although small overall should have implications for the splitting of the various spin-orbit-coupled states arising from the $5f^3$ configuration. Since it is difficult with DFT calculations to isolate the f-orbital space in the complete space of orbitals, an average-of-configurations calculation was performed on **2**. The three unpaired α-electrons were evenly distributed across seven orbitals to produce a set of seven clearly distinct, fractionally occupied f-orbitals. The full decomposition of these orbitals is shown in Table S2. Five of the orbitals show 94-98% 5f character, however two orbitals show much smaller 5f contributions of 62% and 12%, respectively. Summation over the contributions from each 5f orbital to the seven average-of-configuration MOs also shows that the $5f_{z(x^2-y^2)}$, $5f_{xz^2}$, $5f_{x(x^2-3y^2)}$ and $5f_{y(3x^2-y^2)}$ are relatively weakly occupied, with total occupations of 66-79% (Figure S22). This indicates that the splitting of the 5f orbitals in **2** is so strong that it becomes energetically unfavourable in the average-of-configurations calculation to occupy them all, and a partial quenching of the orbital angular momentum occurs.

The electronic structure of **2** creates an interesting juxtaposition with implications for the magnetic properties: whilst donation of electrons from the Cp ligand to the uranium $6d_{yz}$ and $6d_{xz}$ orbitals means that the 5f electrons experience an axial crystal field, the splitting of the 5f orbitals diminishes the anisotropy of the configuration, which impacts on the potential for observing slow magnetic relaxation. To investigate this aspect, the static and dynamic magnetic properties of **[2]**[B(C_6F_5)$_4$] were measured, along with those of **1** for comparative purposes. Firstly, the temperature dependence of $\chi_M T$, where χ_M is the molar magnetic susceptibility, was measured in an applied field of 1 kOe for both compounds. The values of $\chi_M T$ at 300 K are 1.38 cm^3 K mol^{-1} and 1.71 cm^3 K mol^{-1} for **1** and **[2]**[B(C_6F_5)$_4$], respectively, both of which are in the expected range for monometallic uranium(III) compounds.[16] On decreasing the temperature, only a slight decrease in $\chi_M T$ was observed for **1**, with a value of 1.28 cm^3 K mol^{-1} being reached at 2 K (Figure S7). The decrease in $\chi_M T$ with temperature is more pronounced for **[2]**[B(C_6F_5)$_4$], with a sharp drop observed below about 20 K and a value of 0.67 cm^3 K mol^{-1} at 2 K (Figure S9). The field (H) dependence of the magnetization (M) was measured at 2, 3 and 5 K for both compounds, with the same general features being observed. A relatively rapid increase in the magnetization occurs as the field increases to approximately 20 kOe, and at higher fields the increase is more gradual but does not saturate. At 2 K and 70 kOe, **1** and **[2]**[B(C_6F_5)$_4$] attain magnetization values of 1.60 μ_B and 1.10 μ_B, respectively (Figures S9 and S10).

For the oblate spheroidal f-electron density of uranium(III), axially symmetrical environments tend to stabilize crystal field states with large M_J values and, therefore, the ground state can have a large magnetic moment.[17] This situation can lead to field-induced slow magnetic relaxation and occasionally to true single-molecule magnet properties (i.e. without the need for an applied field), although the effective energy barriers (U_{eff}) to reversal of the magnetization are typically very small.[18] This simple design principle has recently been used to great effect in a series of related cationic dysprosium metallocene SMMs, in which the $4f^9$ configuration of Dy^{3+} also has oblate spheroidal electron density.[19] Having established computationally that the $5f^3$ electrons in **2** experience a strong axial crystal field, the possibility of observing slow magnetic relaxation was therefore explored.

Using a small oscillating magnetic field of 5 Oe, zero DC field and frequencies in the range ν = 5-1488 Hz, it was not possible to observe peaks in the temperature dependence of the out-of-phase magnetic susceptibility (χ''_M) for either compound (Figures S11, S16). However, using an optimized field of 1 kOe for **1** and 1.5 kOe for **[2]**[B(C_6F_5)$_4$] (Figures 2, S12-S14, S17-S19), well-defined maxima were observed in the $\chi''_M(\nu)$ plots from 3-6 K for **1** and from 2-5 K for **[2]**[B(C_6F_5)$_4$], with the maxima shifting to higher frequencies as the temperature increases. The lack of slow relaxation in zero field for the two compounds is likely to indicate efficient quantum tunneling of the magnetization (QTM), which is suppressed upon application of a DC field. For the in-field measurements, accurate fits of the temperature dependence of

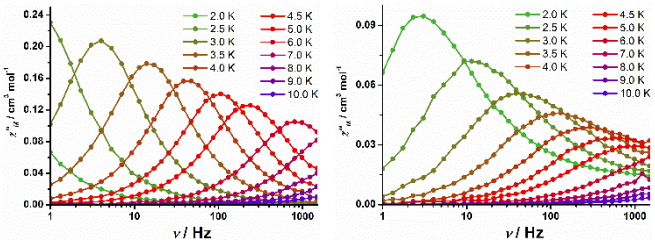

Figure 2. Frequency dependence of χ''_M in **1** (left) and **[2]**[B(C_6F_5)$_4$] (right) at various temperatures, using DC fields of 1 kOe and 1.5 kOe, respectively, and an AC field of 5 Oe.

Accepted Manuscript

This article is protected by copyright. All rights reserved.

10.1002/ange.201903681

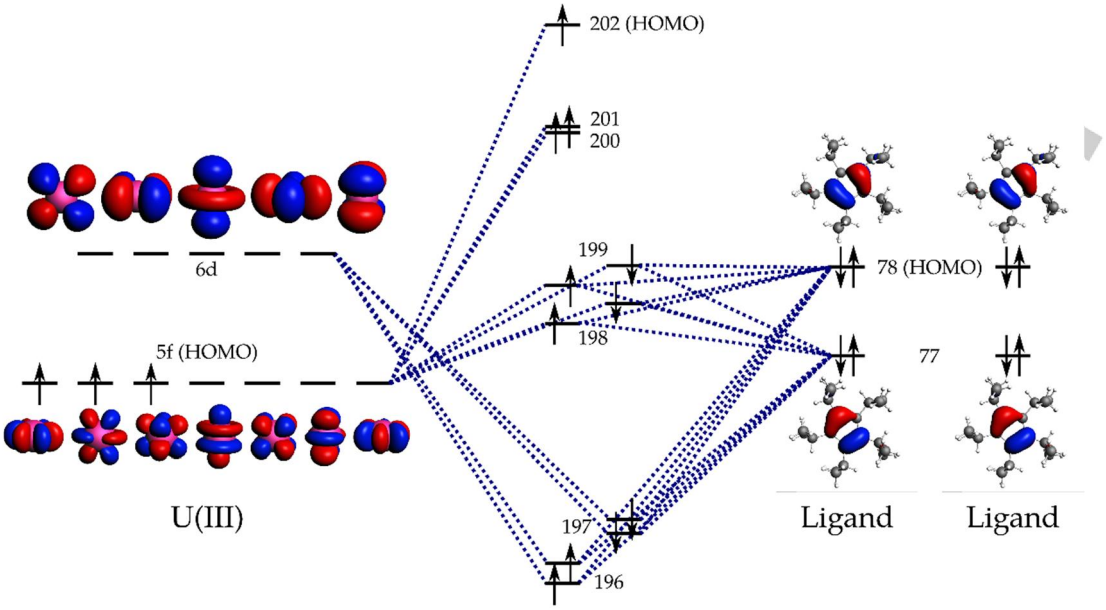

Figure 3. MO diagram for the frontier orbitals of $[(\eta^5\text{-}C_5{}^i\text{Pr}_5)_2\text{U}]^+$ (**2**).

the relaxation time (τ) were obtained for **1** and [**2**][$B(C_6F_5)_4$] using only the Raman expression $\tau^{-1} = CT^n$ in which *C* and *n* are the Raman coefficient and Raman exponent, respectively. The fit parameters are *C* = 0.0033(9) and *n* = 8.1(2), and *C* = 0.26(9) and *n* = 6.4(3), for **1** and for [**2**][$B(C_6F_5)_4$], respectively, with the values of n being typical of an f-element SMM.[19,20] These data indicate that Orbach relaxation processes involving real excited states, such as those commonly observed in dysprosium metallocene SMMs, are not significant in these uranium(III) metallocenes.

To gain further quantitative insight into the electronic structure and magnetism of **2**, a series of multireference ab initio calculations were carried out using the complete active space self-consistent field (CASSCF(3,7)) and restricted active space self-consistent field (RASSCF(15,22)) methods (Figure S23). Importantly, both levels of theory provide qualitatively similar outcomes but with some variations in the quantitative results. This suggests that electron correlation effects cannot be contained in the 5f orbital space, but instead that metal-ligand correlation and covalency are decisive in determining the properties.

At both levels of theory, the ten lowest states, which consist of five Kramers doublets (KDs), form a distinct manifold separated from the next manifold by approximately 2000 cm^{-1}. This is consistent with a $^4I_{9/2}$ ground term with the *J* = 9/2 multiplet split by the crystal field, hence all states relevant to the magnetic properties arise from the $5f^3$ configuration, with other configurations (e.g. $5f^2\ 6d^1$) contributing less than 0.25%. The energies, **g**-tensors, and principal magnetic axes of the five lowest doublets calculated at both levels of theory are listed in Tables S3 and S4. The principal magnetic axis in the ground KD of **2** calculated at the CASSCF(3,7) level (Figure 4) coincides with the pseudo-symmetry axis and passes through the centre of each Cp ligand, with the axes in the higher doublets being close to co-linear. The axis at the RASSCF(15,22) level tilts away from the pseudo-symmetry axis, suggesting that covalency also affect the direction of the principal axis.

All the **g**-tensors have significant transverse components, which explains the lack of slow relaxation in zero field and the need for an external field to suppress the QTM. This is consistent with the metal-ligand covalency breaking the free-ion character of the uranium 5f orbitals and inducing strong mixing of the free-ion terms. Suppression of the QTM allows relaxation to proceed, in principle, via Orbach or Raman processes, however fitting the experimental data requires only a Raman term. This proposal is consistent with the calculations since the two calculated energy gaps between the ground and first-excited KDs (296 cm^{-1} and 366 cm^{-1} at CASSCF(3,7) and RASSCF(15,22)) levels, respectively) would typically correspond to maxima in $\chi''_M(\nu)$ at much higher temperatures that observed for [**2**][$B(C_6F_5)_4$].[12] Furthermore, the difference between the two calculated values is notable, suggesting that the electron correlation effects are not necessarily sufficiently accounted for at these levels of theory. The dependence of calculated KD energies on the level of theory is well known for uranium,[21] which further underscores the importance of covalent factors.

It is instructive to compare the electronic structure and magnetism of **2** with that of its dysprosium analogue $[(\eta^5\text{-Cp*})(\eta^5\text{-}C_5{}^i\text{Pr}_5)\text{Dy}]^+$ (**3**), a high-temperature SMM with a zero-field energy barrier of 1541 cm^{-1} and a blocking temperature of 80 K.[19a] In **3**, the contribution of the $5d_{xz}$ and $5d_{yz}$ orbitals to the metal-ligand interaction is calculated to be 16-19%, *i.e.* similar to the d-orbital participation in **2**. In contrast, the contribution of the 4f orbitals to the valence orbital composition of **3** is 1-4%, i.e. less than half the 5f contribution in **2**. In the average-of-configurations calculation on **3**, the seven 4f orbitals housing the five unpaired β-electrons all feature 4f character of 87-98%, with five orbitals showing more than 96% 4f character. The occupation of all seven 4f orbitals in

Accepted Manuscript

This article is protected by copyright. All rights reserved.

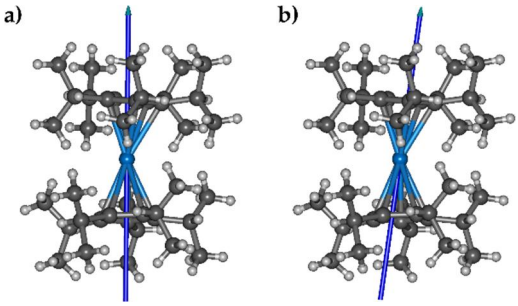

Figure 4. Principal magnetic axis in the ground KD of **2** calculated using CASSCF(3,7) (left) and RASSCF(15,22) (right) methods.

3 is more than 82% with the occupation of five orbitals being more than 96%. Hence, the splitting is very weak, resulting in essentially unquenched orbital angular momentum, strong magnetic anisotropy and the observed SMM properties.

In conclusion, the relatively diffuse uranium 5f orbitals in $[(\eta^5\text{-}C_5{}^iPr_5)_2U]^+$ (**2**) experience strong splitting due to mixing with the ligand orbitals, which leads to appreciable metal-ligand covalency and partially quenches the orbital angular momentum. The impact of this electronic structure is an absence of slow magnetic relaxation in zero field in **2** due to efficient QTM. Therefore, unsymmetrical actinide metallocenes such as uranocenium are unlikely to produce exceptional SMMs, and a more suitable approach would be to enforce orbital degeneracy by designing systems with strict, high point symmetry. From a synthetic perspective, the method developed for **2** may prove to be extendable to sandwich compounds of trans-uranic actinides.

Acknowledgements

We thank the ERC (CoG 646740), the EPSRC (EP/M022064/1), the NSF China (projects 21620102002, 91422302), the National Key Research and Development Program of China (2018YFA0306001), the Magnus Ehrnrooth Foundation, the Academy of Finland (project 289172), the CSC-IT Center for Science in Finland, the Finnish Grid and Cloud Infrastructure (urn:nbn:fi:research-infras-2016072533), and Prof. H. M. Tuononen (University of Jyväskylä) for computational resources.

Keywords: uranium • metallocenes • chemical bonding • electronic structure • magnetic properties

[1] (a) K. L. M. Harriman, M. Murugesu, *Acc. Chem. Res.* **2016**, *49*, 1158. (b) P. L. Arnold, M. S. Dutkiewicz, O. Walter, *Chem. Rev.* **2017**, *117*, 11460. (c) R. P. Kelly, L. Maron, R. Scopelliti, M. Mazzanti, *Angew. Chem. Int. Ed.* **2017**, *56*, 15663. (c) M. Ephritikine, *Organometallics* **2013**, *32*, 2464.

[2] (a) B. E. Bursten, R. J. Strittmatter, *Angew. Chem. Int. Ed.* **1991**, *30*, 1069. (b) T. Hayton, N. Kaltsoyannis, Organometallic Actinide Complexes with Novel Oxidation States, Chapter 4 in *Experimental and Theoretical Approaches to Actinide Chemistry* (Eds J. K. Gibson, W. A. de Jong), Wiley-VCH, Weinheim, **2018**, pp 181-236.

[3] M. Nishiura, F. Guo, Z. Hou, *Acc. Chem. Res.* **2015**, *48*, 2209.

[4] (a) M. Falcone, M. Barluzzi, J. Andrez, F. F. Tirani, I. Zivkovic, A. Fabrizio, C. Corminbeouf, K. Severin, M. Mazzanti, *Nat. Chem.* **2019**, *11*, 154. (b) C. Schoo, S. Bestgen, A. Egberg, S. Klementyeva, C. Feldmann, S. N. Konchenko, P. W. Roesky, *Angew. Chem. Int. Ed.* **2018**, *57*, 5912. (c) N. Tsoureas, A.F. R. Kilpatrick, C. J. Inman, F. G. N. Cloke, *Chem. Sci.* **2016**, *7*, 4624. (d) H. S. La Pierre, K. Meyer, *Prog. Inorg. Chem.* **2014**, *58*, 303.

[5] (a) J. Su, C. J. Windorff, E. R. Batista, W. J. Evans, A. J. Gaunt, M. T. Janicke, S. A. Kozimor, B. L. Scott, D. H. Woen, P. Yang, *J. Am. Chem. Soc.* **2018**, *140*, 7425. (b) B. S. Billow, B. N. Livesay, C. C. Mokhtarzadeh, J. McCracken, M. P. Shores, J. M. Boncella, A. L. Odom, *J. Am. Chem. Soc.* **2018**, *140*, 17369.

[6] (a) C. Zhang, G. Hou, W. Ding, M. Walter, *J. Am. Chem. Soc.* **2018**, *140*, 14511. (b) M. Xémard, S. Zimmer, M. Cordier, V. Goudy, L. Ricard, C. Clavaguéra, G. Nocton, *J. Am. Chem. Soc.* **2018**, *140*, 14433. (c) M. D. Walter, P. Y. Matsunaga, C. J. Burns, L. Maron, R. A. Andersen, *Organometallics* **2017**, *36*, 4564.

[7] (a) A. Streitweiser Jr., U. Mueller-Westerhoff, *J. Am. Chem. Soc.* **1968**, *90*, 7364. (b) A. Zalkin, K. N. Raymond, *J. Am. Chem. Soc.* **1969**, *91*, 5667.

[8] K. N. Raymond, *New. J. Chem.* **2015**, 39, 7540.

[9] (a) N. Magnani, C. Apostolidis, A. Morgenstern, E. Colineau, J.-C. Griveau, H. Bolvin, O. Walter, R. Caciuffo, *Angew. Chem. Int. Ed.* **2011**, *50*, 1696. (b) S. G. Minasian, J. M. Keith, E. R. Batista, K. S. Boland, D. L. Clark, S. A. Kozimor, R. L. Martin, D. K. Shuh, T. Tyliszczak, *Chem. Sci.* **2014**, *5*, 351.

[10] D.-C. Sergentu, F. Gendron, J. Autschbach, *Chem. Sci.* **2018**, *9*, 6292.

[11] (a) M. Ephritikhine, *Dalton Trans.* **2006**, 2501. (b) J. Maynadié, N. Barros, J.-C. Berthet, P. Thuéry, L. Maron, M. Ephritikhine, *Angew. Chem. Int. Ed.* **2007**, *46*, 2010.

[12] B. M. Day, F.-S. Guo, R. A. Layfield, *Acc. Chem. Res.* **2018**, *51*, 1880. (b) A. Gaita-Ariño, F. Luis, E. Coronado, S. Hill, *Nat. Chem.* **2019**, *11*, 301.

[13] S. J. Connelly, W. Kaminsky, D. M. Heinekey, *Organometallics* **2013**, *32*, 7478.

[14] CCDC reference codes 1898062 and 1898063.

[15] (a) ADF2017. SCM, Theoretical Chemistry, Vrije Universiteit Amsterdam, The Neatherlands. http://www.scm.com. 2017. (b) G. te Velde, F. M. Bickelhaupt, E. J. Baerendes, C. Fonseca Guerra, S. J. A. Gisbergen, J. G. Snijders, T. Ziegler, *J. Comp. Chem.* **2001**, *22*, 931. (c) C. Fonseca Guerra, J. G. Snijders, G. te Velde, E. J. Baerends, *Theor. Chem. Acc.* **1998**, *99*, 391.

[16] H. S. La Pierre, A. Scheurer, F. W. Heinemann, W. Hieringer, K. Meyer, *Angew. Chem. Int. Ed.* **2014**, *53*, 7158.

[17] (a) D. R. Kindra, W. J. Evans, *Chem. Rev.* **2014**, *114*, 8865. (b) F. Moro, D. P. Mills, S. T. Liddle, J. van Slageren, *Angew. Chem. Int. Ed.* **2013**, *52*, 3430.

[18] (a) J. J. Le Roy, S. I. Gorelsky, I. Korobkov, M. Murugesu, *Organometallics* **2015**, *34*, 1415. (b) K. R. Meihaus, S. Minasian, W. W. Lukens Jr., S. A. Kozimor, D. K. Shuh, T. Tyliszczak, J. R. Long, *J. Am. Chem. Soc.* **2014**, *136*, 6056. (c) J. D. Rinehart, J. R. Long, *Dalton Trans.* **2012**, *41*, 13572. (d) K. R. Meihaus, J. D. Rinehart, J. R. Long, *Inorg. Chem.* **2011**, *50*, 8484. (e) K. R. Meihaus, J. R. Long, *Dalton Trans.* **2015**, *44*, 2517.

[19] (a) F.-S. Guo, B. M. Day, Y.-C. Chen, M.-L. Tong, A. Mansikkamäki, R. A. Layfield, *Science*, **2018**, *362*, 1400. (b) K. R. McClain, C. A. Gould, K. Chakarawet, S. J. Teat, T. J. Groshens, J. R. Long, B. G. Harvey, Chem. Sci. **2018**, *9*, 8492. (c) F.-S. Guo, B. M. Day, Y.-C. Chen, M.-L. Tong, A. Mansikkamäki, R. A. Layfield, *Angew. Chem., Int. Ed.* **2017**, *56*, 11445. (d) C. A. P. Goodwin, F. Ortu, D. Reta, N. F. Chilton, D. P. Mills, Nature, **2017**, *548*, 439.

[20] S. T. Liddle, J. van Slageren, Actinide Single-Molecule Magnets, Chapter 10 in *Lanthanide and Actinides in Molecular Magnetism* (Eds R. A. Layfield, M. Murugesu) Wiley-VCH, Weinheim, 2015, pp 315-339.

[21] J. T. Coutinho, M. Perfetti, J. J. Baldoví, M. A. Antunes, P. P Hallmen, H. Bamberger, I. Crassee, M. Orlita, M. Almeida, J. van Slageren, L. C. J. Pereira, *Chem. Eur. J.* **2019**, *25*, 1758.

Accepted Manuscript

This article is protected by copyright. All rights reserved.

10.1002/ange.201903681

WILEY-VCH

Entry for the Table of Contents

COMMUNICATION

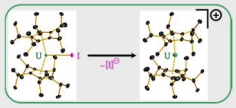

Fu-Sheng Guo, Yan-Cong Chen, Ming-Liang Tong, Akseli Mansikkamäki,* Richard A. Layfield**

Page No. – Page No.

Uranocenium: Synthesis, Structure and Chemical Bonding

Uranium sandwiches. Appreciable covalency in a uranocenium cation involving 5f and 6d orbitals partially quenches the orbital angular momentum and leads to slow magnetic relaxation via a Raman mechanism.

WILEY-VCH Accepted Manuscript

This article is protected by copyright. All rights reserved.